Research Square

Preprints are preliminary reports that have not undergone peer review.
They should not be considered conclusive, used to inform clinical practice,
or referenced by the media as validated information.

Dynamic and Non-Thermodynamic Processes Dominate Extreme Monsoon Rainfall Intensification at the Eastern Himalayan Margin

Laldinchhuaha Khiangte[1]

khiangtedinchhuaha@gmail.com

Mizoram University

Michelle Lalhruaizeli[2]

Mizoram University

Vishwambhar Prasad Sati[1]

Mizoram University

B. P. Mishra[2]

Mizoram University

Article

Keywords: Extreme precipitation, South Asian monsoon, atmospheric dynamics, Clausius-Clapeyron scaling, Mizoram, ERA5, CMIP6

Posted Date: July 9th, 2026

DOI: https://doi.org/10.21203/rs.3.rs-10231180/v1

License: This work is licensed under a Creative Commons Attribution 4.0 International License.
Read Full License

Additional Declarations: No competing interests reported.

Title

Dynamic and Non-Thermodynamic Processes Dominate Extreme Monsoon Rainfall Intensification at the Eastern Himalayan Margin

Authors

Laldinchhuaha Khiangte[1]*, Michelle Lalhruaizeli[2], Vishwambhar Prasad Sati[1], B. P. Mishra[2]

Affiliations

[1] Department of Geography and Resource Management, Mizoram University, Aizawl 796004, Mizoram, India

[2] Department of Environmental Science, Mizoram University, Aizawl 796004, Mizoram, India

*Corresponding author: Laldinchhuaha Khiangte

khiangtedinchhuaha@gmail.com

ORCID: https://orcid.org/0009-0003-3258-7299

Acknowledgements

The authors gratefully acknowledge the India Meteorological Department (IMD) for providing the long-term gridded rainfall dataset used in this study. We also acknowledge the European Centre for Medium-Range Weather Forecasts (ECMWF) and the Copernicus Climate Change Service (C3S) for providing the ERA5 reanalysis dataset. CMIP6 historical simulations were accessed through the Copernicus Climate Data Store (CDS), and we thank the modelling groups participating in CMIP6 for producing and making their simulations publicly available.

Funding

This research received no specific grant from any funding agency in the public, commercial, or not-for-profit sectors.

Declaration of Competing Interest

The authors declare that they have no known competing financial interests or personal relationships that could have appeared to influence the work reported in this paper.

Abstract

Extreme precipitation is projected to intensify under climate warming in accordance with Clausius–Clapeyron scaling, yet the extent to which atmospheric circulation modulates this response remains uncertain, particularly across mountainous monsoon environments. Here, we examine a 125-year daily rainfall record from Mizoram, situated within the Indo-Myanmar Ranges along the eastern margin of the South Asian monsoon, in combination with ERA5 reanalysis and selected CMIP6 historical simulations. Annual maximum 1-day precipitation (Rx1day) increased by 27% following an abrupt regime shift during the mid-1970s, while total annual rainfall exhibited no statistically significant long-term change. Notably, this intensification occurred despite a marked decline in the 850 hPa horizontal moisture flux after 2003. A simple thermodynamic decomposition indicates that local Clausius–Clapeyron scaling accounts for only approximately 16% of the observed increase in Rx1day, leaving the remaining 84% unexplained by thermodynamic scaling and therefore more likely attributable to dynamic and other non-thermodynamic processes. The absence of a significant interannual relationship between extreme precipitation and local temperature further suggests that thermodynamic forcing alone is insufficient to account for the observed changes. Collectively, these results imply that projections relying primarily on thermodynamic scaling may underestimate future increases in extreme rainfall across mountainous monsoon regions, where atmospheric circulation and complex topography exert a dominant influence on precipitation extremes. Improving the representation of convection and terrain–atmosphere interactions in climate models is therefore essential for reducing uncertainty in projections of extreme rainfall at the margins of the South Asian monsoon.

Keywords: Extreme precipitation; South Asian monsoon; atmospheric dynamics; Clausius-Clapeyron scaling; Mizoram; ERA5; CMIP6.

1. Introduction

The response of the hydrological cycle to anthropogenic climate warming is among the most societally significant consequences of climate change. A fundamental thermodynamic expectation is that extreme precipitation should intensify at a rate of approximately 7% per degree Celsius of warming, as described by the Clausius-Clapeyron relationship (Held & Soden, 2006; O'Gorman & Schneider, 2009). Although this scaling is broadly supported by global and mid-latitude

observations (Arias et al., 2021), its applicability over tropical land, particularly within monsoon systems, remains uncertain (Utsumi et al., 2011; Ali & Mishra, 2017). In these regions, moisture availability for heavy rainfall depends not only on local temperature but also on large-scale atmospheric circulation that transports moisture from distant oceanic source regions. Consequently, changes in atmospheric circulation, convective organisation, and orographic uplift can equal or, in some settings, exceed the contribution of thermodynamic warming to changes in extreme precipitation (Pfahl et al., 2017; Bao et al., 2017).

The South Asian monsoon provides a clear example of this complexity. Across the Indian subcontinent, several studies have documented a decoupling between mean monsoon rainfall and precipitation extremes, with heavy rainfall events becoming more frequent and intense alongside declining mean monsoon rainfall across parts of central and northern India since the mid-twentieth century (Goswami et al., 2006; Roxy et al., 2015 ; Samantray & Gouda 2024). Previous studies have attributed these changes to a combination of thermodynamic influences, including increasing atmospheric moisture content, and dynamic changes such as a weakening of the large-scale monsoon circulation and shifts in the frequency and intensity of synoptic weather systems (Krishnan et al., 2016; Ajayamohan et al., 2010). However, most existing studies have focused on central and western India, whereas the eastern margin of the South Asian monsoon, encompassing the steep and densely forested Indo-Myanmar Ranges, remains comparatively understudied despite its exceptional susceptibility to landslides, flash floods, and hydrological hazards (Nadim et al., 2006).

Mizoram is located in the Indo-Myanmar (Burma) Ranges at the eastern margin of the Himalayan-Tibetan orogenic system, exemplifies this important knowledge gap. The region receives more than 2,000 mm of average annual rainfall generated through the combined influence of Bay of Bengal moisture transport, complex orography, and mesoscale convective systems (Houze, 2012). Despite these characteristics, it remains unclear whether extreme rainfall has undergone significant long-term changes during the instrumental period and, if so, whether those changes are primarily consistent with thermodynamic warming or are more strongly influenced by atmospheric circulation. Addressing this question is important not only for regional hazard assessment but also for improving our understanding of how mountainous monsoon regions, which remain among the

most uncertain areas in future precipitation projections, may respond to continued climate warming (Li et al., 2021).

In this study, we address this gap using one of the longest available continuous daily rainfall records for the region, spanning 125 years (1901–2025). We combine this record with ERA5 reanalysis diagnostics and a CMIP6 historical ensemble to (i) quantify trends and regime shifts in extreme precipitation, (ii) identify the large-scale circulation changes associated with the observed shifts, (iii) compare the observed changes against model-estimated natural variability, and (iv) partition the observed change into its thermodynamic and dynamic components. The central questions are whether extreme monsoon rainfall has changed over the instrumental period in this eastern Himalayan margin, and, if so, whether the change is primarily driven by local thermodynamic scaling or by shifts in atmospheric circulation. Given the well-documented decoupling between mean and extreme monsoon rainfall over India, we hypothesize that circulation-driven (dynamic) processes account for a substantial fraction of the observed intensification, beyond what is expected from thermodynamic warming alone. Our results support this view and carry direct implications for adaptation in mountainous monsoon regions worldwide.

2. Results

2.1 Annual and seasonal context

Mizoram's mean annual rainfall for 1901-2025 is 2,226 mm, but the interannual variability is large (s.d. = 382 mm). Over the full period, annual rainfall shows no statistically significant trend (MMK $p = 0.21$; Sen's slope = 1.21 mm yr^{-1}). This gross stability, however, conceals a pronounced seasonal reorganisation. Monsoon (June–September) rainfall has increased significantly (slope = 1.77 mm yr^{-1}, $p = 0.017$), while winter (January-February) rainfall has declined (slope = −0.14 mm yr^{-1}, $p = 0.037$; Fig. 1a and Supplementary Fig. S1). The monsoon season now supplies roughly 64% of the annual total, up from its early twentieth century share, meaning the region's water availability has become more tightly compressed into a narrower, more intense monsoon window.

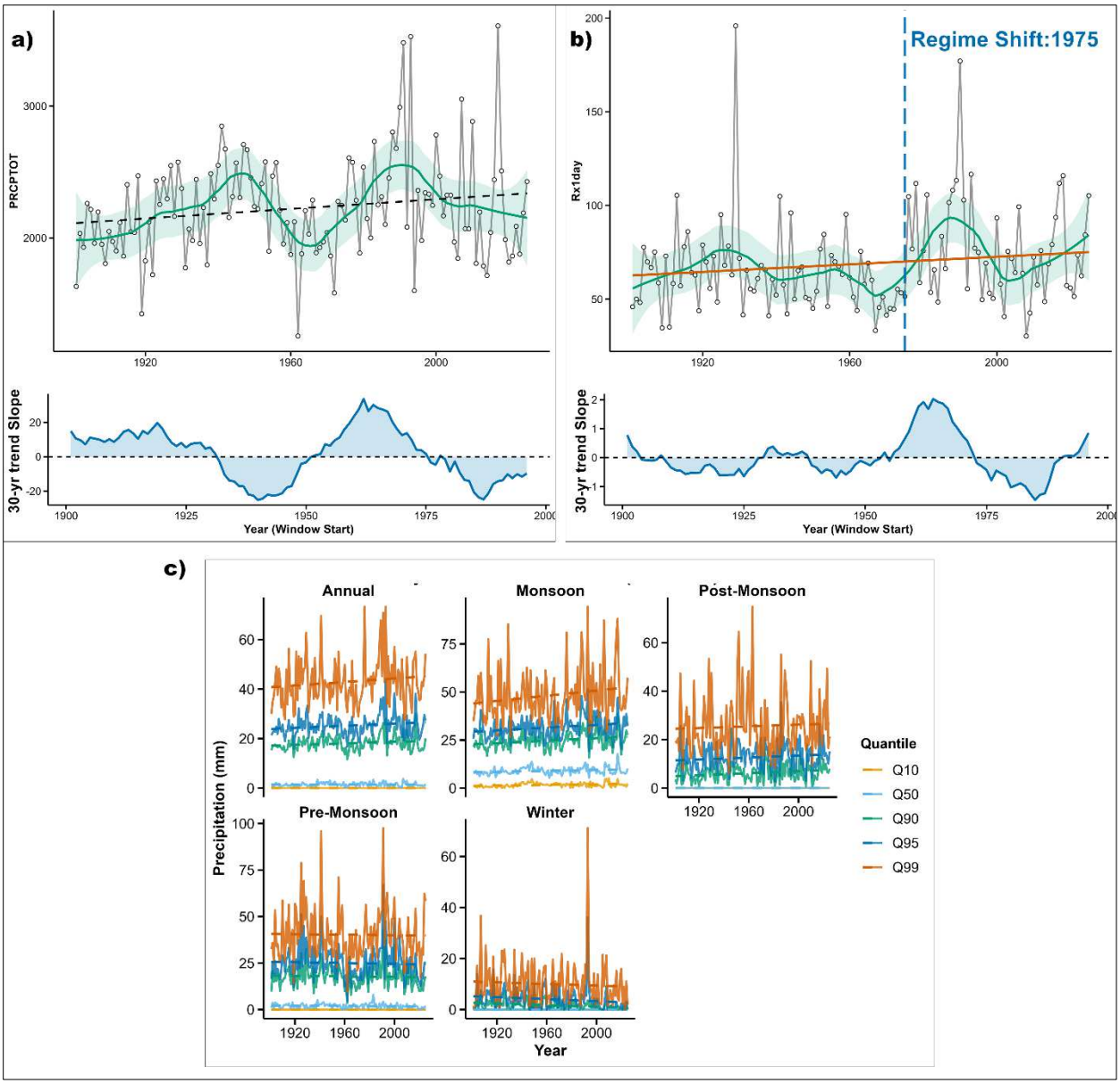


Figure 1. Observed extreme-rainfall intensification over Mizoram.

a) *Annual total precipitation (PRCPTOT) for 1901–2025 with a loess smoother and Sen's trend (dashed line).* ***b)*** *Annual maximum 1-day precipitation (Rx1day). A Pettitt breakpoint is detected in 1975 (vertical dashed line); the solid red line shows the significant Sen's trend.* ***c)*** *Quantile trends of daily monsoon (June–September) rainfall. The median (Q50) is stable while Q90 and Q99 rise. All data from the IMD 0.25° gridded dataset averaged over Mizoram (22–24° N, 92–93° E). n = 125 years.*

2.2 Intensification of extreme daily rainfall

Every index that captures the intensity of heavy rain shows a significant upward trend (Fig. 1b; Supplementary Table S1). The annual maximum 1-day precipitation (Rx1day) increased by 0.08 mm yr^{-1} (MMK $p = 0.028$), the contribution from very wet days (R95p) by 0.90 mm yr^{-1} ($p = 0.010$), and that from extremely wet days (R99p) by 0.34 mm yr^{-1} ($p = 0.034$). The simple daily intensity index (SDII) also rose (0.006 mm day^{-1} yr^{-1}, $p = 0.046$). At the same time, neither the maximum duration of consecutive wet days (CWD) nor consecutive dry days (CDD) exhibited significant trends, and the occurrence of moderate or severe meteorological drought (SPI-3) also remained unchanged ($p > 0.5$; Supplementary Fig. S5). Overall, the persistence of wet and dry spells remained broadly stable, whereas the intensity of the heaviest rainfall events increased significantly.

2.3 A mid-1970s regime shift

These changes are not the tail end of a gradual drift; they reflect an abrupt reorganisation. Pettitt change-point tests identify a significant break in the mid-1970s for the key extreme-rainfall indices: 1975 for Rx1day ($p = 0.014$), R99p ($p = 0.029$), and SDII ($p = 0.033$; Supplementary Table S1). The Buishand test independently places a break at 1975 for the same variables. Bayesian change-point analysis yields a sharp peak in posterior probability around 1975 for both Rx1day and R95p (Supplementary Fig. S2). Running 30-year trends (the WMO standard climatological period) confirm that the strongest positive slopes in extreme indices are concentrated in windows centred on the 1960s-1970s (Supplementary Fig. S3). For the monsoon season as a whole, a break is detected earlier (~1937), but the extreme-indices break is tightly clustered around 1975.

2.4 Tail fattening without a shift in the centre

Quantile regression reveals a clear pattern: the median daily rainfall has not changed (Q50 slope ≈ 0, $p = 0.89$), whereas the upper tail has become markedly heavier. The 90th percentile increased by 0.058 mm yr^{-1} ($p < 0.001$), the 95th percentile by 0.086 mm yr^{-1}, and the 99th percentile by 0.107 mm yr^{-1} ($p = 0.023$; Fig. 1c). In the monsoon season the same pattern holds, with all quantiles above the median trending positive. Winter shows the opposite a significant decline in the 90th percentile. The result is a “fattening” of the upper tail of the daily rainfall distribution, concentrated in the monsoon months. A stationary generalized extreme value (GEV) model was preferred over a non-stationary formulation (Supplementary Fig. S4), indicating that the annual maximum series

has not yet undergone a detectable shift in its underlying extreme-value distribution. Full quantile regression results for all seasons are provided in Supplementary Table S2.

2.5 Persistence and long-range memory

Hurst exponents for all extreme indices lie in the range 0.52–0.68, well above the 0.5 threshold for white noise (Supplementary Table S3). This long-range persistence means that wet and dry epochs tend to persist over decades, consistent with the multi-decadal trend reversals seen in the running-window analysis. However, long-range memory does not by itself establish the permanence of any specific change point; it indicates that the post-1975 shift is part of a low-frequency reorganisation of the monsoon system rather than a short-lived fluctuation.

2.6 Large-scale circulation changes associated with extreme rainfall intensification

To investigate the large-scale atmospheric changes associated with the observed increase in extreme rainfall, ERA5 reanalysis data (1950-2025) were analysed. The most prominent circulation change is a significant decrease in the 850 hPa horizontal moisture flux magnitude over Mizoram, with an abrupt drop around 2003 (Pettitt $p = 0.007$; Fig. 2a). The post-2003 flux is, on average, 11% lower than the pre-2003 mean. Neither seasonal mean moisture convergence nor mid-tropospheric vertical velocity (500 hPa ω) exhibited a significant change point. The composite difference map (Fig. 2b) reveals a weakening of the south-westerly flow from the Bay of Bengal directly over the region. The combination of stronger extreme rainfall and weaker mean low-level moisture transport initially appears counter-intuitive. This pattern suggests that the observed intensification cannot be explained solely by an increase in the mean moisture supply and is consistent with more efficient conversion of available moisture into intense precipitation. Although not directly evaluated here, changes in convective organisation, orographic lifting, or synoptic-scale forcing represent physically plausible mechanisms.

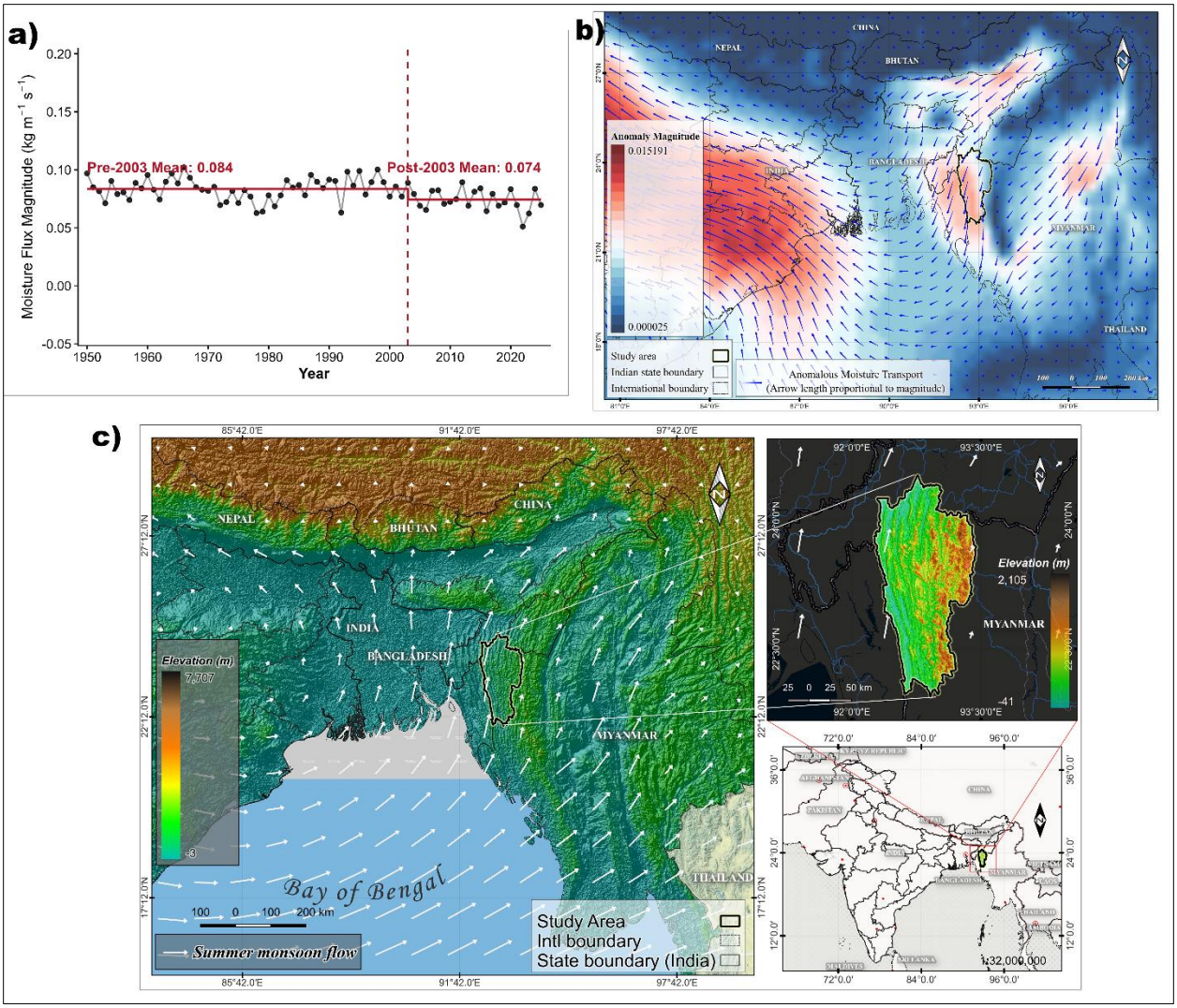


Figure 2. Large-scale circulation changes associated with the observed intensification of extreme rainfall.

a) *Time series of the JJAS mean 850 hPa horizontal moisture flux magnitude averaged over Mizoram during 1950–2025. A Pettitt test identifies a significant change point in 2003, and the horizontal lines indicate the mean moisture flux before and after the change point.* ***b)*** *Composite difference in 850 hPa horizontal moisture flux (post-2003 minus pre-2003). Colours show the magnitude of the moisture-flux anomaly, while arrows indicate changes in the horizontal moisture-flux vectors, illustrating the weakening of southwesterly moisture transport over northeast India. The red box outlines Mizoram.* ***c)*** *Regional topographic setting showing the study area (red box), the CMIP6 extraction domain (dashed blue box), and the climatological summer monsoon flow*

from the Bay of Bengal. This panel illustrates the topographic and circulation setting through which Bay of Bengal moisture is transported towards Mizoram. All circulation diagnostics were derived from ERA5 monthly reanalysis data.

2.7 Comparison against model-estimated natural variability

We compared the observed Rx1day against a two-model CMIP6 historical ensemble (EC-Earth3 and MPI-ESM1-2-HR) that realistically simulates precipitation over the narrow Mizoram domain. The pre-1975 ensemble spread (29-101 mm) is used as a proxy for internal variability. After 1975, 22.5% of observed years exceed the pre-1975 95th percentile, and 30% exceed the 90th percentile, compared with the expected 5% and 10% (Fig. 3a). The observed mean Rx1day increased from 59.2 mm before 1975 to 75.4 mm thereafter (27%), whereas the corresponding multi-model mean exhibited little change over the same period. The distribution of observed Rx1day has visibly shifted to the right (Fig. 3b).

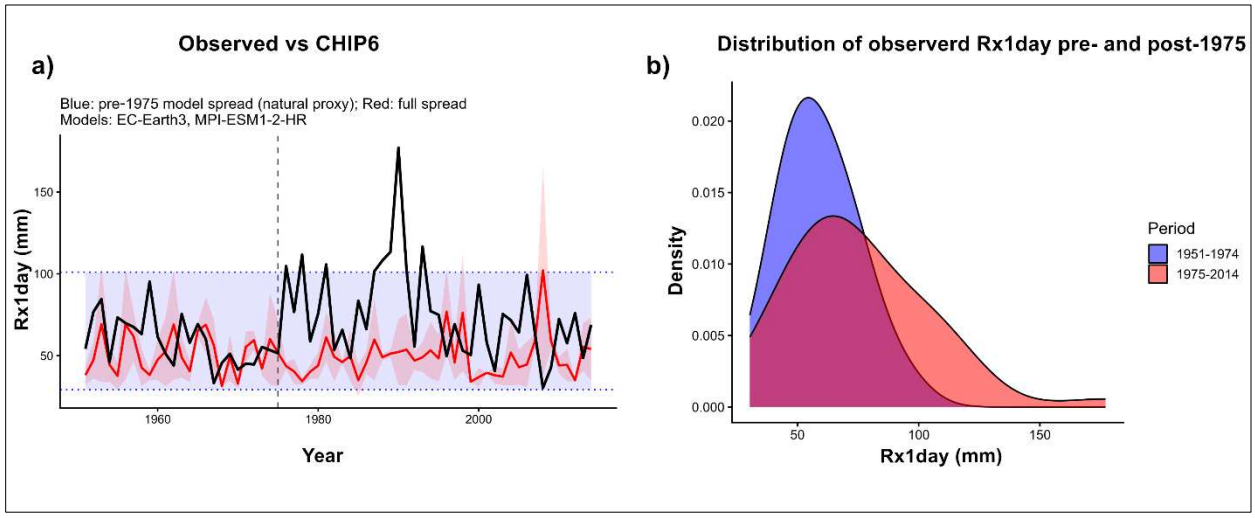


Figure 3. Comparison of observed Rx1day with CMIP6 model-estimated natural variability.

a) *Observed annual Rx1day (black line) for 1951–2014 compared with the CMIP6 historical ensemble. The red line denotes the two-model ensemble mean (EC-Earth3 and MPI-ESM1-2-HR), while the red shading indicates the ensemble 5–95% range. The blue shaded band represents the pre-1975 ensemble 5–95% range, used as a proxy for model-estimated natural variability.* ***b)*** *Density distributions of observed Rx1day before (blue) and after (red) 1975. Model*

indices were extracted with a 3×3 grid-cell mean centred on Mizoram (91.6–93.4° E, 22.1–24.0° N).

2.8 Thermodynamic and dynamic contributions

We quantified the thermodynamic contribution to the observed increase using the Clausius-Clapeyron relation. Regional monsoon-season (JJAS) near-surface air temperature rose by 0.63 °C between the pre-1975 and post-1975 periods. Applying the theoretical scaling of 7% $°C^{-1}$ to the pre-1975 mean Rx1day yields an expected thermodynamic increase of 2.6 mm, which is only 16% of the total observed change (Fig. 4a). The remaining 84% is not explained by local thermodynamic scaling and likely arises from dynamic and other non-thermodynamic processes. This decomposition is consistent with the absence of any significant interannual correlation between Rx1day and local temperature ($\beta = -2.5\%\ °C^{-1}$, $p = 0.77$; Fig. 4c), and with the negative relationship between 30-year temperature and Rx1day trends ($p = 0.002$; Fig. 4b). Even the direct scaling with lower-tropospheric specific humidity yields only a weak, non-significant sensitivity (21.5% per g kg^{-1}, $p = 0.38$). These multiple lines of evidence strongly suggest that dynamic and other non-thermodynamic processes play a dominant role in the intensification of extreme rainfall over Mizoram.

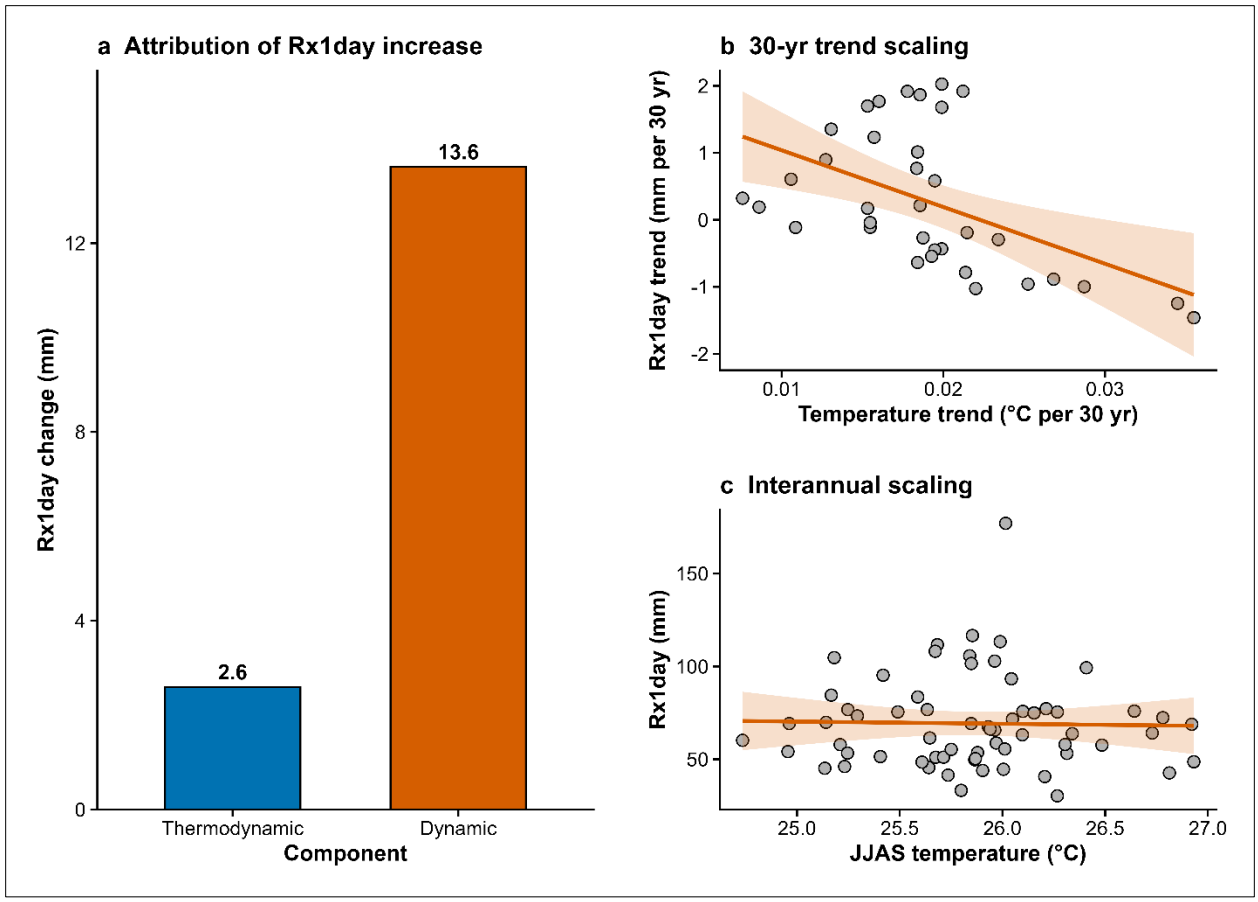


Figure 4 *.* ***Thermodynamic and dynamic contributions to the observed Rx1day increase.*** ***a,*** *Two-component decomposition of the total Rx1day change. The thermodynamic contribution (blue) is estimated from the observed 0.63 °C regional warming and Clausius–Clapeyron scaling (7% °C⁻¹); the residual (red) reflects dynamic and other non-thermodynamic processes.* ***b,*** *Relationship between 30-year trends in JJAS temperature and Rx1day. Sen's slopes of overlapping 30-year windows; the red line is a linear fit (p = 0.002).* ***c,*** *Interannual scaling of observed Rx1day with JJAS temperature (1951–2014). The fitted line (β = –2.5% °C⁻¹, p = 0.77) shows no significant relationship. All temperature data from ERA5 (JJAS, 2-m air temperature). Error bands are ±1 s.e.m.*

3. Discussion

Our analysis of a 125-year rainfall record reveals that extreme monsoon precipitation over Mizoram has intensified substantially while total annual rainfall has remained unchanged. The key signal is a 27% increase in the annual maximum 1-day precipitation (Rx1day) that commenced

abruptly in the mid-1970s, coincident with a significant fattening of the upper tail of the daily rainfall distribution (Fig. 1). This shift occurred in the absence of any significant increase in the low-level moisture flux; on the contrary, the 850 hPa horizontal moisture flux magnitude declined significantly after 2003 (Fig. 2). A two-component decomposition indicates that only 16% of the observed increase can be explained by the local thermodynamic response to warming, while the remaining 84% likely arises from dynamic and other non-thermodynamic processes (Fig. 4). Together, these findings strongly suggest a dominant role for circulation-driven changes in the intensification of extreme rainfall at the eastern Himalayan margin.

The notion that extreme precipitation should scale with atmospheric moisture content-roughly 7% per degree of warming according to the Clausius-Clapeyron relation-is now a cornerstone of climate change projections (Held & Soden, 2006; O'Gorman & Schneider, 2009). Yet a growing body of evidence suggests that this simple thermodynamic scaling often fails over tropical land, especially in monsoon regions where moisture availability is tightly coupled to large-scale dynamics (Utsumi et al., 2011; Ali & Mishra, 2017). Over India, earlier work demonstrated a decoupling between mean and extreme monsoon rainfall, with the frequency and intensity of heavy events rising despite an overall drying trend in central and northern India since the 1950s (Goswami et al., 2006; Roxy et al., 2015; Vinod & Mahesha, 2024). Our results extend this paradigm to the monsoon's eastern margin, where the dynamic contribution so substantially outweighs the thermodynamic one that the temperature-based scaling is almost absent on interannual time scales (Fig. 4c). This finding is consistent with recent global analyses showing that the interannual scaling of extreme precipitation with surface temperature is weak or even negative over tropical and subtropical monsoon domains, where moisture-transport convergence rather than local moisture-holding capacity governs rainfall intensity (Pendergrass et al., 2017; Bao et al., 2017).

Although not directly evaluated in this study, several physically plausible mechanisms may explain the observed regime shift. The 1970s saw a well-documented phase change in the Pacific Decadal Oscillation and a concomitant reorganisation of the Asian monsoon circulation (Trenberth, 1990; Annamalai et al., 2013). It also marked the beginning of a rapid increase in Asian aerosol emissions, particularly from the Indian subcontinent, which are known to alter the meridional thermal gradient and affect monsoon dynamics (Bollasina et al., 2011; Wang et al., 2009).

Absorbing aerosols may strengthen the pre-monsoon land-sea contrast and invigorate convection over northeast India, while simultaneously reducing the total moisture flux through solar dimming and surface cooling (Sanap et al., 2015). The subsequent decline in South Asian aerosol emissions after the early 2000s, driven by clean-air policies, may have further modified the circulation, contributing to the observed weakening of the 850 hPa moisture flux after 2003 (Samset et al., 2018). This scenario-an aerosol-induced shift in convective regime in the 1970s followed by a greenhouse gas driven thermodynamic amplification and a later dynamic response to aerosol reductions is physically plausible and testable in single-forcing CMIP6 experiments, although such experiments are beyond the scope of the present study.

The importance of dynamics for extreme rainfall in this region has immediate implications for future projections. Global climate models consistently project a strengthening of extreme precipitation under continued warming (Arias et al., 2021), but the magnitude and even the sign of the monsoon circulation response remain highly uncertain (Wang et al., 2020). Our results imply that projections that rely primarily on thermodynamic arguments the assumption that "wet gets wetter" may substantially underestimate the risk of intensifying monsoon extremes in mountainous margins where orographic uplift and mesoscale organisation amplify the effect of even modest circulation changes. The steep topography of the Indo-Myanmar Ranges, which concentrates moisture flux over a narrow corridor, likely plays a critical role in translating a dynamical signal into a disproportionate increase in local extreme rainfall (Houze, 2012). From a hazard perspective, the intensification we document translates directly into a heightened risk of landslides and flash floods, as the same annual water volume is being delivered in a smaller number of more intense events. This shift is not captured by standard drought or flood indices that rely on monthly or seasonal totals, and may therefore be hidden from managers who monitor only mean precipitation (Peduzzi et al., 2012).

Several limitations must be acknowledged. First, our comparison against model-estimated natural variability relies on a two-model CMIP6 ensemble because three out of five available models fail to resolve the narrow Mizoram land-sea mask, placing the grid point over the ocean and yielding zero annual maxima. While the retained models (EC-Earth3 and MPI-ESM1-2-HR) realistically simulate monsoon precipitation in the region, a larger ensemble would better constrain the natural variability baseline. Second, the study area is a single small state, and the extent to which the

results generalise to other mountainous monsoon margins such as the Western Ghats, the Arakan coast of Myanmar, or the Himalayan foothills remains to be tested. A wider spatial analysis using the IMD 0.25° gridded dataset across Northeast India is a logical next step. Third, our decomposition uses a simple, fixed 7% $°C^{-1}$ thermodynamic scaling; in reality, the scaling may vary regionally and across time scales, and the residual therefore encapsulates all processes not captured by this constant, including internal variability and model uncertainty. Finally, while we have discussed a plausible aerosol-driven mechanism, we have not performed a formal single-forcing attribution analysis, which would be required to definitively ascribe the 1975 shift to a specific forcing.

Despite these limitations, the coherence of the signal across multiple independent lines of evidence observed trends, change-point tests, quantile regression, reanalysis circulation diagnostics, and model-based comparison and attribution provides strong confidence that the intensification of extreme precipitation over Mizoram is robust, abrupt, and is most consistently explained by dynamic and other non-thermodynamic processes. The study underscores the need for convection-permitting regional climate simulations and process-oriented model evaluation over monsoon margins, where the interaction between large-scale dynamics and complex orography creates a unique and under-studied extreme-rainfall regime. In a warming world, understanding the dynamic component of extreme precipitation change is not merely an academic exercise; it is essential for building resilient infrastructure and early-warning systems in the world's most vulnerable mountain communities.

4. Data and Methods

4.1 Observed rainfall data

Daily gridded rainfall at 0.25° × 0.25° resolution for India was obtained from the India Meteorological Department (IMD) for the period 1901-2025 (Pai et al., 2014). The dataset has been operationally extended beyond 2010 using the same interpolation and quality-control procedures. All grid cells whose centroids lie within the boundaries of Mizoram (approximately 22–24° N, 92–93° E) were spatially averaged to produce a single daily time series for the state. Data homogeneity was assessed with the Pettitt, Buishand, and standard normal homogeneity tests (Pettitt, 1979; Buishand, 1982). Annual and seasonal totals were computed for winter (January-

February), pre-monsoon (March-May), monsoon (June-September, JJAS), and post-monsoon (October-December), consistent with standard Indian meteorological seasons. No missing daily rainfall values were present in the IMD gridded dataset over the study period.

4.2 Extreme precipitation indices

The 27 core indices of the Expert Team on Climate Change Detection and Indices (ETCCDI) were calculated using the R package climdex.pcic (Zhang et al., 2011). The analysis focused on the annual maximum 1-day precipitation (Rx1day), the contribution from very wet and extremely wet days (R95p, R99p and their fractions of annual total), the simple daily intensity index (SDII), consecutive dry days (CDD), and consecutive wet days (CWD). A 3-month Standardized Precipitation Index (SPI-3) was used to characterise meteorological drought (McKee et al., 1993).

4.3 Trend, change-point and persistence analysis

Monotonic trends were evaluated with the Mann-Kendall (MK) test and the magnitude of the trend was estimated with Sen's slope (Mann, 1945; Kendall, 1975; Sen, 1968). For a time series $x_1, x_2, \dots, x_n$, the MK statistic S is

$$S = \sum_{i=1}^{n-1} \sum_{j=i+1}^{n} \operatorname{sgn}(x_j - x_i) \tag{1}$$

where $\operatorname{sgn}(\theta) = 1, 0, -1$ for $\theta > 0, = 0, < 0$. The variance of S is

$$\operatorname{Var}(S) = \frac{1}{18}\left[n(n-1)(2n+5) - \sum_{p=1}^{q} t_p\,(t_p-1)(2t_p+5)\right] \tag{2}$$

with q tied groups and t_p the number of data points in the p-th group. The standardised test statistic Z is then

$$Z = \begin{cases} (S-1)/\sqrt{\operatorname{Var}(S)} & S > 0 \\ 0 & S = 0 \\ (S+1)/\sqrt{\operatorname{Var}(S)} & S < 0 \end{cases} \tag{3}$$

Sen's slope is the median of all pairwise slopes $(x_j - x_i)/(j - i)$ for $i < j$. Serial correlation was accounted for with the modified Mann-Kendall test (Hamed & Rao, 1998) and the trend-free pre-whitening procedure (Yue et al., 2002).

Abrupt regime shifts were detected with the Pettitt test (Pettitt, 1979). The Pettitt statistic K is defined as the position where the split between two sub-samples maximises the rank-based comparison:

$$K = \max_{1 \le t < n} \left| \sum_{i=1}^{t} \sum_{j=t+1}^{n} \operatorname{sgn}(x_i - x_j) \right| \quad (4)$$

The significance of K is assessed against the null hypothesis of no change point. The Buishand range test (Buishand, 1982) and a Bayesian change-point analysis (Barry & Hartigan, 1993) were used to confirm the breakpoints. Long-range persistence was quantified with the Hurst exponent estimated by detrended fluctuation analysis (Kantelhardt et al., 2002). A 30-year moving window was adopted because it corresponds to the standard World Meteorological Organization climatological normal and is widely used for assessing multi-decadal climate variability. Unless otherwise stated, statistical significance was assessed at $\alpha = 0.05$.

4.4 Quantile regression and extreme-value analysis

Trends across the distribution of daily rainfall were assessed using quantile regression (Koenker & Bassett, 1978). The conditional quantile model $Q_\tau(Y \mid t) = \beta_0(\tau) + \beta_1(\tau)t$ was fitted for the 10th, 50th, 90th, 95th, and 99th percentiles (τ) of annual and seasonal precipitation, with year (t) as the explanatory variable. Statistical significance of the regression coefficients was evaluated using the default inference procedure implemented in the R package *quantreg*. Non-stationarity in the annual maximum rainfall series was evaluated by fitting both stationary and non-stationary generalized extreme value (GEV) distributions, with the location parameter allowed to vary linearly with time (Coles, 2001). Model performance was compared using a likelihood-ratio test.

4.5 Large-scale circulation and moisture flux

To investigate the atmospheric processes associated with the observed changes in extreme rainfall, monthly mean ERA5 reanalysis data (Hersbach et al., 2020) were obtained for 1950–2023 on pressure levels (u- and v-wind, specific humidity at 850 hPa; vertical velocity at 500 hPa) and single levels (mean sea level pressure). JJAS seasonal means were computed. Horizontal moisture flux at 850 hPa was calculated as (qu, qv), where q is specific humidity and u and v are the zonal and meridional wind components. The area-averaged 850 hPa moisture-flux magnitude over Mizoram was then computed. Moisture convergence was estimated from the horizontal divergence of the 850 hPa moisture-flux components using centred finite differences on the native ERA5 grid. Pettitt tests were applied to the area-averaged flux magnitude, moisture convergence, and 500 hPa vertical velocity to detect abrupt dynamical changes.

4.6 Comparison with CMIP6 historical simulations and thermodynamic-dynamic decomposition

Yearly Rx1day values were extracted from the "Climate extreme indices and heat stress indicators" dataset (C3S, version 2.0) for the historical experiment of the Coupled Model Intercomparison Project Phase 6 (CMIP6; Eyring et al., 2016). After quality filtering, two models that realistically simulate precipitation over the narrow Mizoram land strip were retained: EC-Earth3 and MPI-ESM1-2-HR (one ensemble member each, r1i1p1f1). The pre-1975 (1951–1974) 5-95% spread of the multi-model ensemble served as a natural-variability baseline; the observed Rx1day was compared against this envelope.

The thermodynamic contribution to the observed change in Rx1day was estimated using the Clausius-Clapeyron scaling of approximately 7% per degree Celsius of warming (Held & Soden, 2006):

$$\Delta R_{\text{thermo}} = \bar{R}_{\text{pre-1975}} \times 0.07 \times \Delta T \quad (5)$$

where ΔT is the post-1975 minus pre-1975 change in JJAS near-surface air temperature (ERA5). The residual component, representing processes not explained by Clausius–Clapeyron thermodynamic scaling (including dynamic and other non-thermodynamic influences), was calculated as the difference between the observed and thermodynamically expected changes. In addition, the interannual scaling of Rx1day with JJAS temperature and with 850 hPa specific

humidity was examined with ordinary least-squares regression, and the scaling of 30-year trends was assessed using Sen's slope on overlapping 30-year windows.

4.7 Software

All computations were performed in R (R Core Team, 2025) using the packages *trend, modifiedmk, quantreg, extRemes, bcp, SPEI, fractal, and ggplot2*. ERA5 and CMIP6 data retrieval used the *ecmwfr* package. Processed data and analysis scripts are available from the corresponding author upon reasonable request.

5. Conclusion

By analysing a 125-year rainfall record together with atmospheric reanalyses and climate model simulations, our analyses suggest that the observed intensification of extreme monsoon precipitation over the eastern Himalayan margin is dominated by dynamic and other non-thermodynamic processes. Although total annual rainfall over Mizoram has remained statistically unchanged, the annual maximum 1-day precipitation (Rx1day) increased by 27% following an abrupt regime shift in the mid-1970s. At the same time, the most intense rainfall events became systematically heavier, whereas the number of wet days and the frequency of meteorological drought showed no significant long-term changes. A simple Clausius-Clapeyron scaling indicates that only approximately 16% of the observed increase can be explained by local thermodynamic warming, while the remaining 84% is not explained by thermodynamic scaling and is therefore likely associated with dynamic and other non-thermodynamic processes.

Importantly, the intensification of extreme rainfall occurred despite a significant weakening of the 850 hPa horizontal moisture flux after approximately 2003. This initially counter-intuitive combination of stronger precipitation extremes and weaker mean low-level moisture transport suggests that the atmosphere has become more efficient at converting available moisture into intense rainfall, potentially through changes in convective organisation, orographic enhancement, or synoptic-scale circulation. Furthermore, the absence of a significant interannual relationship between extreme precipitation and either near-surface air temperature or lower-tropospheric specific humidity is consistent with the conclusion that thermodynamic forcing alone cannot explain the observed changes.

These findings have important implications for future climate projections and regional risk assessment. Climate models that rely primarily on thermodynamic scaling may underestimate future changes in extreme rainfall over mountainous monsoon regions, where relatively small circulation changes can be substantially amplified by complex terrain. From a hazard-management perspective, the concentration of a similar annual rainfall total into fewer but more intense precipitation events is likely to increase the risk of flash floods and landslides, hazards that are not adequately represented by indices based solely on seasonal or annual precipitation totals. Continued improvements in the representation of convection, moisture transport, and terrain-atmosphere interactions within climate models, together with process-oriented model evaluation, are therefore essential for reducing uncertainty in projections of extreme rainfall in these vulnerable environments.

Although the present study focuses on a single mountainous monsoon region, the analytical framework developed here provides a basis for investigating whether similar changes are occurring elsewhere along the eastern Himalayan arc and other topographically complex monsoon regions, including the Western Ghats. Extending this approach using consistent observational datasets, complemented by dedicated single-forcing climate model experiments, would help determine whether the predominance of dynamic and other non-thermodynamic processes identified here represents a broader characteristic of South Asian monsoon margins. Such efforts would contribute to a more complete understanding of the mechanisms governing future changes in extreme precipitation under a warming climate.

Data availability

Daily gridded rainfall data were obtained from the India Meteorological Department (IMD). ERA5 reanalysis data were obtained from the Copernicus Climate Change Service, and CMIP6 simulations were obtained through the Earth System Grid Federation (ESGF). Owing to the licensing terms of the IMD dataset, these data are not redistributed through this repository and should be obtained directly from the respective data providers.

Code availability

The R scripts used to reproduce the analyses presented in this study, along with the associated processed data files, are publicly available on GitHub at https://github.com/DinosKuri/mizoram-

extreme-rainfall-attribution and are permanently archived on Zenodo (https://doi.org/10.5281/zenodo.21132748).

References

1. Ajayamohan, R. S., Merryfield, W. J., & Kharin, V. V. (2010). Increasing trend of synoptic activity and its relationship with extreme rain events over central India. *Journal of Climate, 23*(4), 1004–1013. https://doi.org/10.1175/2009JCLI2918.1
2. Ali, H., & Mishra, V. (2017). Contrasting response of rainfall extremes to increase in surface air and dewpoint temperatures at urban locations in India. *Scientific Reports, 7*, Article 1228. https://doi.org/10.1038/s41598-017-01306-1
3. Annamalai, H., Hafner, J., Sooraj, K. P., & Pillai, P. (2013). Global warming shifts the monsoon circulation, drying South Asia. *Journal of Climate, 26*(8), 2701–2718. https://doi.org/10.1175/JCLI-D-12-00208.1
4. Arias, P. A., Bellouin, N., Coppola, E., Jones, R. G., Krinner, G., Marotzke, J., Naik, V., Palmer, M. D., Plattner, G.-K., Rogelj, J., Rojas, M., Sillmann, J., Storelvmo, T., Thorne, P. W., Trewin, B., Achuta Rao, K., Adhikary, B., Armour, K., Bala, G., ... Zickfeld, K. (2021). Technical summary. In V. Masson-Delmotte, P. Zhai, A. Pirani, S. L. Connors, C. Péan, S. Berger, N. Caud, Y. Chen, L. Goldfarb, M. I. Gomis, M. Huang, K. Leitzell, E. Lonnoy, J. B. R. Matthews, T. K. Maycock, T. Waterfield, O. Yelekçi, R. Yu, & B. Zhou (Eds.), *Climate change 2021: The physical science basis. Contribution of Working Group I to the Sixth Assessment Report of the Intergovernmental Panel on Climate Change* (pp. 33–144). Cambridge University Press. https://doi.org/10.1017/9781009157896.002
5. Bao, J., Sherwood, S. C., Alexander, L. V., & Evans, J. P. (2017). Future increases in extreme precipitation exceed observed scaling rates. *Nature Climate Change, 7*(2), 128–132. https://doi.org/10.1038/nclimate3201
6. Barry, D., & Hartigan, J. A. (1993). A Bayesian analysis for change point problems. *Journal of the American Statistical Association, 88*(421), 309–319. https://doi.org/10.1080/01621459.1993.10594328
7. Bollasina, M. A., Ming, Y., & Ramaswamy, V. (2011). Anthropogenic aerosols and the weakening of the South Asian summer monsoon. *Science, 334*(6055), 502–505. https://doi.org/10.1126/science.1204994

8. Buishand, T. A. (1982). Some methods for testing the homogeneity of rainfall records. *Journal of Hydrology, 58*(1–2), 11–37. https://doi.org/10.1016/0022-1694(82)90066-X
9. Coles, S. (2001). *An introduction to statistical modeling of extreme values*. Springer.
10. Eyring, V., Bony, S., Meehl, G. A., Senior, C. A., Stevens, B., Stouffer, R. J., & Taylor, K. E. (2016). Overview of the Coupled Model Intercomparison Project Phase 6 (CMIP6) experimental design and organization. *Geoscientific Model Development, 9*(5), 1937–1958. https://doi.org/10.5194/gmd-9-1937-2016
11. Goswami, B. N., Venugopal, V., Sengupta, D., Madhusoodanan, M. S., & Xavier, P. K. (2006). Increasing trend of extreme rain events over India in a warming environment. *Science, 314*(5804), 1442–1445. https://doi.org/10.1126/science.1132027
12. Hamed, K. H., & Rao, A. R. (1998). A modified Mann–Kendall trend test for autocorrelated data. *Journal of Hydrology, 204*(1–4), 182–196. https://doi.org/10.1016/S0022-1694(97)00125-X
13. Held, I. M., & Soden, B. J. (2006). Robust responses of the hydrological cycle to global warming. *Journal of Climate, 19*(21), 5686–5699. https://doi.org/10.1175/JCLI3990.1
14. Hersbach, H., Bell, B., Berrisford, P., Hirahara, S., Horányi, A., Muñoz Sabater, J., Nicolas, J., Peubey, C., Radu, R., Schepers, D., Simmons, A., Soci, C., Abdalla, S., Abellan, X., Balsamo, G., Bechtold, P., Biavati, G., Bidlot, J., Bonavita, M., ... Thépaut, J.-N. (2020). The ERA5 global reanalysis. *Quarterly Journal of the Royal Meteorological Society, 146*(730), 1999–2049. https://doi.org/10.1002/qj.3803
15. Houze, R. A., Jr. (2012). Orographic effects on precipitating clouds. *Reviews of Geophysics, 50*(1), RG1001. https://doi.org/10.1029/2011RG000365
16. Kantelhardt, J. W., Zschiegner, S. A., Koscielny-Bunde, E., Havlin, S., Bunde, A., & Stanley, H. E. (2002). Multifractal detrended fluctuation analysis of nonstationary time series. *Physica A: Statistical Mechanics and Its Applications, 316*(1–4), 87–114. https://doi.org/10.1016/S0378-4371(02)01383-3
17. Kendall, M. G. (1975). *Rank correlation methods* (4th ed.). Charles Griffin.
18. Koenker, R., & Bassett, G. (1978). Regression quantiles. *Econometrica, 46*(1), 33–50. https://doi.org/10.2307/1913643
19. Krishnan, R., Sabin, T. P., Vellore, R., Mujumdar, M., Sanjay, J., Goswami, B. N., Hourdin, F., Dufresne, J.-L., Terray, P., & Boos, W. R. (2016). Deciphering the desiccation

trend of the South Asian monsoon hydroclimate in a warming world. *Climate Dynamics, 47*(3–4), 1007–1027. https://doi.org/10.1007/s00382-015-2886-5

20. Mann, H. B. (1945). Nonparametric tests against trend. *Econometrica, 13*(3), 245–259. https://doi.org/10.2307/1907187
21. McKee, T. B., Doesken, N. J., & Kleist, J. (1993). *The relationship of drought frequency and duration to time scales*. In *Proceedings of the 8th Conference on Applied Climatology* (pp. 179–184). American Meteorological Society.
22. Nadim, F., Kjekstad, O., Peduzzi, P., Herold, C., & Jaedicke, C. (2006). Global landslide and avalanche hotspots. *Landslides, 3*(2), 159–173. https://doi.org/10.1007/s10346-006-0036-1
23. O'Gorman, P. A., & Schneider, T. (2009). The physical basis for increases in precipitation extremes in simulations of 21st-century climate change. *Proceedings of the National Academy of Sciences, 106*(35), 14773–14777. https://doi.org/10.1073/pnas.0907610106
24. Pai, D. S., Sridhar, L., Rajeevan, M., Sreejith, O. P., Satbhai, N. S., & Mukhopadhyay, B. (2014). Development of a new high spatial resolution (0.25° × 0.25°) long period (1901–2010) daily gridded rainfall data set over India and its comparison with existing data sets over the region. *Mausam, 65*(1), 1–18. https://doi.org/10.54302/mausam.v65i1.851
25. Pendergrass, A. G., Knutti, R., Lehner, F., Deser, C., & Sanderson, B. M. (2017). Precipitation variability increases in a warmer climate. *Scientific Reports, 7*(1), Article 17966. https://doi.org/10.1038/s41598-017-17966-y
26. Pettitt, A. N. (1979). A nonparametric approach to the change-point problem. *Journal of the Royal Statistical Society: Series C (Applied Statistics), 28*(2), 126–135. https://doi.org/10.2307/2346729
27. Pfahl, S., O'Gorman, P. A., & Fischer, E. M. (2017). Understanding the regional pattern of projected future changes in extreme precipitation. *Nature Climate Change, 7*(6), 423–427. https://doi.org/10.1038/nclimate3287
28. R Core Team. (2025). *R: A language and environment for statistical computing*. R Foundation for Statistical Computing. https://www.R-project.org/
29. Roxy, M. K., Ritika, K., Terray, P., Masson, S., & Sooraj, K. P. (2015). Drying of Indian subcontinent by rapid Indian Ocean warming and a weakening land–sea thermal gradient. *Nature Communications, 6*, Article 7423. https://doi.org/10.1038/ncomms8423

30. Samantray, P., & Gouda, K. C. (2024). A review on the extreme rainfall studies in India. *Natural Hazards Research, 4*(3), 347–356. https://doi.org/10.1016/j.nhres.2023.08.005
31. Samset, B. H., Sand, M., Smith, C. J., Bauer, S. E., Forster, P. M., Fuglestvedt, J. S., O'Neill, B. C., & Schleussner, C.-F. (2018). Climate impacts from a removal of anthropogenic aerosol emissions. *Geophysical Research Letters, 45*(2), 1020–1029. https://doi.org/10.1002/2017GL076079
32. Sanap, S. D., Pandithurai, G., & Manoj, M. G. (2015). On the response of Indian summer monsoon to aerosol forcing in CMIP5 model simulations. *Climate Dynamics, 45*(9–10), 2949–2961. https://doi.org/10.1007/s00382-015-2516-2
33. Sen, P. K. (1968). Estimates of the regression coefficient based on Kendall's tau. *Journal of the American Statistical Association, 63*(324), 1379–1389. https://doi.org/10.1080/01621459.1968.10480934
34. Trenberth, K. E. (1990). Recent observed interdecadal climate changes in the Northern Hemisphere. *Bulletin of the American Meteorological Society, 71*(7), 988–993. https://doi.org/10.1175/1520-0477(1990)071%3C0988:ROICCI%3E2.0.CO;2
35. Utsumi, N., Seto, S., Kanae, S., Maeda, E. E., & Oki, T. (2011). Does higher surface temperature intensify extreme precipitation? *Geophysical Research Letters, 38*(16), L16708. https://doi.org/10.1029/2011GL048426
36. Vinod, D., & Mahesha, A. (2024). Large-scale atmospheric teleconnections and spatiotemporal variability of extreme rainfall indices across India. *Journal of Hydrology, 628*, 130584. https://doi.org/10.1016/j.jhydrol.2023.130584
37. Wang, B., Jin, C., & Liu, J. (2020). Understanding future change of global monsoons projected by CMIP6 models. *Journal of Climate, 33*(15), 6471–6489. https://doi.org/10.1175/JCLI-D-19-0993.1
38. Wang, C., Kim, D., Ekman, A. M. L., Barth, M. C., & Rasch, P. J. (2009). Impact of anthropogenic aerosols on Indian summer monsoon. *Geophysical Research Letters, 36*(21), L21704. https://doi.org/10.1029/2009GL040114
39. Yue, S., Pilon, P., Phinney, B., & Cavadias, G. (2002). The influence of autocorrelation on the ability to detect trend in hydrological series. *Hydrological Processes, 16*(9), 1807–1829. https://doi.org/10.1002/hyp.1095

572 40. Zhang, X., Alexander, L., Hegerl, G. C., Jones, P., Tank, A. K., Peterson, T. C., Trewin,
573 B., & Zwiers, F. W. (2011). Indices for monitoring changes in extremes based on daily
574 temperature and precipitation data. *WIREs Climate Change, 2*(6), 851–870.
575 https://doi.org/10.1002/wcc.147

Supplementary Files

This is a list of supplementary files associated with this preprint. Click to download.

- Supplementarymaterial.docx